Mon. Not. R. Astron. Soc. **000**, 1–9 (2015) Printed 13 January 2016 (MN LATEX style file v2.2)

Jiamusi Pulsar Observations: I. Abnormal emission events of PSR B0919+06

Jun Han[1,4], J. L. Han[1 ⋆], Ling-Xiang Peng[2,3], De-Yu Tang[2], Jun Wang[2], Jun-Qiang Li[2], Chen Wang[1,3], Ye-Zhao Yu[1,4], Bin Dong[1,3]

[1]*National Astronomical Observatories, Chinese Academy of Sciences, Jia-20 Datun Road, ChaoYang District, Beijing 100012, China*
[2]*Jiamusi Deep Space Station, China Xi'an Satellite Control Center, Jiamusi, Heilongjiang 154002, China*
[3]*The State Key Laboratory of Astronautic Dynamics, Xi'an, Shaanxi 710043, China*
[4]*School of Astronomy, University of Chinese Academy of Sciences, Beijing 100049, China*

arXiv:1601.02889v1 [astro-ph.HE] 12 Jan 2016

Accepted 2015 December 03. Received 2015 December 02; in original form 2015 October 30

ABSTRACT

PSR B0919+06 generally radiates radio pulses in a normal phase range. It has been known for its occasional perplexing abnormal emission events wherein individual pulses come to an earlier phase range for a few tens of periods and then returns to its usual phase. Heretofore, only a few such events have been available for study. We observed PSR B0919+06 for about 30 hours using the Jiamusi 66-m telescope at Jiamusi Deep Space Station at S-band, and detected 92 abnormal emission events. We identify four types of events based on the abrupted or gradual phase-shifting of individual pulses. The abnormal emission events are seen to occur randomly some every 1000 to 3000 periods, and they affect the leading edge of the mean profile by up to 2% in amplitude. The abnormal emission events are probably related to gradual changes of emission processing in the pulsar magnetosphere.

Key words: pulsars: general – pulsars: individual: PSR B0919+06.

1 INTRODUCTION

Pulsars radiate the pulsed emission periodically, though individual pulses vary in shape and in intensity. Sub-pulses of individual pulses can appear in different ranges of pulsar rotation phases. Various phenomena such as nulling, subpulse drifting and mode-changing have been observed from many pulsars (see e.g. Sobey et al. 2015). When individual pulses are averaged over many periods, the mean pulse profile is very stable for a pulsar in general, which is believed to be a cut of the emission window of pulsar magnetosphere (Manchester 1995), and their polarization features are closely related to the emission geometry (e.g. Lyne & Manchester 1988; Gangadhara & Gupta 2001; Wang et al. 2013). Sub-pulses of some pulsars drift within the pulsar emission window (e.g. Rankin 1986; Rankin et al. 2013). Some pulsars exhibit different emission modes in a sequence of individual pulses. For example, the precursor of the main pulse and the interpulse of PSR B1822−09 are relevantly switched on and off for several hundreds of periods (Gil et al. 1994; Latham et al. 2012). The extreme case for emission mode changes is the nulling phenomena, in which case the emission process appears to be fully stopped for many periods (e.g. Wang et al. 2007; Yang et al. 2014; Sobey et al. 2015).

PSR B0919+06 is a nearby bright pulsar with a period of 0.43062 s and a small dispersion measure of 27.27 pc cm^{-3} (Hobbs et al. 2009). Its narrow mean pulse profile at high frequencies (e.g. above 1.4 GHz) is highly polarized (Stinebring et al. 1984; Johnston et al. 2008; Hankins & Rankin 2010), and is very asymmetric with a long gradual leading edge and a sharp trailing edge. Such a profile was classified as a partial cone by Lyne & Manchester (1988), and the emission at high frequencies originates mainly from the trailing conal component. At lower frequencies, two or three profile components emerge (Phillips & Wolszczan 1992; Smits et al. 2006; Johnston et al. 2008; Hankins & Rankin 2010), and the central core and leading conal components become stronger. Orthogonal polarization modes have been observed mainly in the central weak component (Stinebring et al. 1984; Rankin et al. 2006; Smits et al. 2006).

The abnormal emission events of PSR B0919+06 were first discovered by Rankin et al. (2006), who noticed five occurrences of a gradual shifting of individual pulses about 5° in longitude towards early pulse phases from four pulse squences of 10763 pulses in total. From their observations made on MJD 52854 at 1425 MHz, two abnormal emission events are seen in the pulse series of 480 s (1115 pulses), each lasting for 30-40 periods with a separation of some 650 periods. Rankin et al. (2006) observed PSR B0919+06 at 327 MHz for 30 minutes (4180 pulses) on MJD 52916, and detected one event lasting for 60 periods. They also found two more abnormal emission events in archive data of Stinebring et al. (1984)

⋆ E-mail: hjl@nao.cas.cn

© 2015 RAS

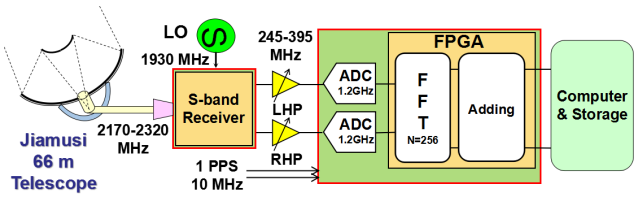

Figure 1. The system used for observations. See text for explanations.

Table 1. Observational parameters for PSR B0919+06.

Obs. Date UTC	MJD	Start Time UTC	Obs. length min. / Pulse No.	Channel No.	Sample (ms)
2015.04.18	57130	13:29	15.0 / 2088	256	0.19968
2015.07.12	57215	04:09	381.0 / 53053	256	0.19968
2015.07.14	57217	01:07	485.2 / 67611	256	0.19968
2015.08.17	57251	22:31	466.5 / 65003	128	0.09984
2015.08.18	57252	22:15	253.4 / 35306	256	0.19968
2015.08.19	57253	03:20	179.4 / 25001	256	0.19968

of 3582 pulses observed on MJD 44857 at 1.4 GHz, but no event from 1886 pulses observed on MJD 44859. The great advantage of the observations made by Rankin et al. (2006) is that polarization data are recorded. The orthogonal polarization modes and the integrated polarization profiles for the normal emission mode and the abnormal emission events of PSR B0919+16 obtained from these observations clearly show that the leading conal component and the core component emerge during the abnormal emission events at 1425 MHz and during the normal the abnormal modes at 327 MHz. The orthogonal polarization modes were detected from not only the core component at 1425 MHz but also both the leading conal component and the core component at 327 MHz. A very important conclusion derived from the observation of Rankin et al. (2006) is that the polarization angles during the abnormal emission events follow the same "S"shaped-curve as the trailing conal component (shown in their Figure 3) after the orthogonal polarization modes are considered, suggesting that the abnormal emission events occur as if the two profile components at early pulse phases are lightened and the trailing conal component is switched off.

Such abnormal emission events of PSR B0919+06 for a gradual shifting of individual pulses were recently confirmed by Perera et al. (2015) from their single pulses observed at MJD 55751. In addition to such a so-called "main flare state" of 5° shifting Perera et al. (2015) found a "small flare state", characterized by a smaller gradual shifting of about 3° in longitude of pulse phases for a few seconds.

Very intriguing is the fact that the profiles of PSR B0919+06 have also shown two states (Lyne et al. 2010; Perera et al. 2015) with the most distinctive difference exactly in the range of pulse phases where abnormal emission events stand out. Long term timing observations of PSR B0919+06 (Lyne et al. 2010; Perera et al. 2015) show that its spin-down rate $\dot{\nu}$ varies between "low and high states" with a double-peak structure and a quasi-periodicity of 630 days or 550 days, which was seen to be very closely correlated with variations between the two profile states. Perera et al. (2015) removed the identified "flare states" shown in one or two subintegrations (10 seconds or 1 minute each) from their timing data of normally 20 minutes and found that the correlation still exists between the slow $\dot{\nu}$ variations and the profile-shape parameters. It is possible that variations of profiles arised from either some unidentified "flare states" or the leakages of flares to nearby subintegrations or "small flares" in their timing data.

At the present, it is unclear how often and how long the abnormal emission events occur in PSR B0919+06 and how much they contribute to the profile variations. Here we report our observations of PSR B0919+06 for about 30 hours by using the Jiamusi 66-m telescope at Jiamusi Deep Space Station, in which we find 92 abnormal emission events. The observation system is briefly described in Sect. 2, the results are presented and analyzed in Sect. 3, and discussions and conclusions are given in Sect. 4.

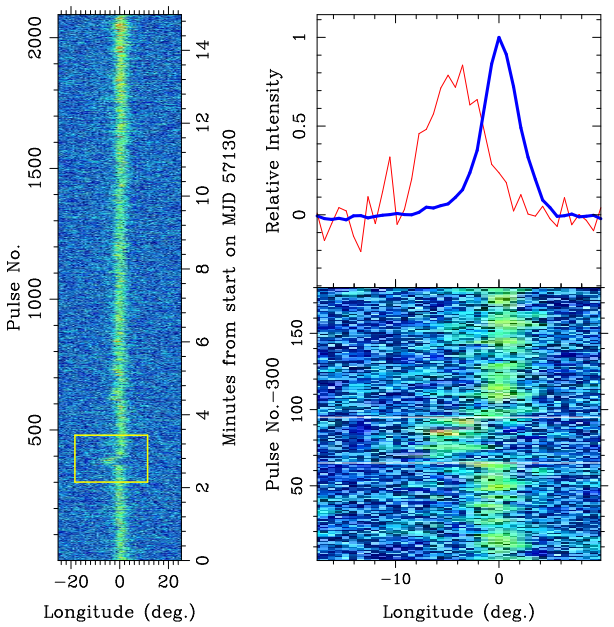

Figure 2. Results from a test observation of PSR B0919+06 on MJD 57130. The left panel shows a plot of 2088 individual pulses observed in 15 minutes. An enlarged plot for 180 pulses, including an abnormal emission event between the pulses numbers 365 and 395, is shown in the right-bottom panel. The comparison of mean profiles for the normal emission mode (thick line) and abnormal emission event (thin line) are shown in the top-right panel.

2 THE OBSERVATION SYSTEM AND DATA TAKING

The Jiamusi 66-m telescope is located at Jiamusi in Heilongjiang province, China, which is operated by the Jiamusi Deep Space Station of the China Xi'an Satellite Control Center. A cryogenically cooled dual-channel S-band receiver was used for the observations, which has a bandwidth of about 140 MHz at the radio frequency around 2.25 GHz. After adjusting the signal amplitude of the intermediate frequency (IF) output with two variable-gain amplifiers, we connected a digital backend to the receiver (see Figure 1 for illustration). The backend samples the IF signals and then channelizes the signals via a FFT module in a Field-Programmable Gate Array (FPGA) board. The total radio power is obtained by summing the detected power from the left hand and right hand polarization receivers for each of the 256 or 128 frequency channels, and then accumulated for duration of the sampling time. The accumulated radio powers of 256 or 128 channels are saved to a computer with a time resolution of 0.2 ms or 0.1 ms.

A test observation was made for 15 minutes on 2015 April 18

Table 2. A list of abnormal emission events for detailed plots

MJD	Event No.	Start–End pulse No.	Duration	Type	Details
57130	1	365 – 395	31	Π	Fig.2
57215	1	1360 – 1400	41	?	Fig.12
57215	2	2940 – 2975	36	M	Fig.9
57215	3	4638 – 4683	46	M	Fig.9
57215	4	6710? – 6760	51	M	Fig.9
57215	5	9510 – 9550	41	?	Fig.12
57215	6	15280? – 15325?	46	?	Fig.12
57215	7	18258 – 18309	52	Π	Fig.8
57215	8	20238 – 20284	47	Π	Fig.8
57215	9	22040 – 22080	41	Π	Fig.8
57215	10	23213 – 23248	36	λ	Fig.11
57215	11	24315 – 24339	25	Λ	Fig.10
57215	12	27330? – 27365?	36?	?	Fig.12
57215	13	29845 – 29882?	38?	M	Fig.9
57215	14	31422 – 31460	39	M	Fig.9
57215	15	33130 – 33163	34	M	Fig.9
57215	16	35195 – 35240	46	M	Fig.9
57215	17	43770 – 43812	43	?	Fig.12
57215	18	46745 – 46794	50	Π	Fig.8
57215	19	48722 – 48770	49	Π	Fig.8
57215	20	50525 – 50567	43	Π	Fig.8
57215	21	51700 – 51736	37	λ	Fig.11
57215	22	52796 – 52822	27	Λ	Fig.10
57217	1	3175 – 3225?	51?	M	Fig.9
57217	2	4900? – 4935?	36?	?	Fig.12
57217	3	14950 – 14993	44	M	Fig.9
57217	4	16955 – 16990	36	M	Fig.9
57217	5	21495 – 21535	41	?	Fig.12
57217	6	31165? – 31190?	26?	Λ	Fig.10
57217	7	33278 – 33312	35	M	Fig.9
57217	8	35414 – 35449	36	M	Fig.9
57217	9	38315 – 38357	43	M	Fig.9
57217	10	39651 – 39690	40	M	Fig.9
57217	11	39982 – 39998	17	Λ	Fig.10
57217	12	40777 – 40796	20	Λ	Fig.10
57217	13	42208 – 42250	43	M	Fig.9
57217	14	44078 – 44127	50	M	Fig.9
57217	15	46200 – 46235	36	?	Fig.12
57217	16	53655 – 53700	46	M	Fig.9
57217	17	55047 – 55080	34	M	Fig.9
57217	18	61080 – 61120	41	λ	Fig.11
57217	19	63446 – 63482	37	M	Fig.9
57217	20	65035? – 65070?	36?	?	Fig.12
57217	21	66840 – 66875	36	?	Fig.12
57251	1	1050? – 1090?	41?	?	Fig.12
57251	2	5522 – 5565	44	M	Fig.9
57251	3	6860 – 6887	28	Λ	Fig.10
57251	4	8125 – 8165?	41?	M	Fig.9
57251	5	14750? – 14780?	31?	?	Fig.12
57251	6	16170 – 16195	26	?	Fig.12
57251	7	22020? – 22055	36?	M	Fig.9
57251	8	23822 – 23856	35	Λ	Fig.10
57251	9	25867 – 25903	37	M	Fig.9
57251	10	28397 – 28436	40	M	Fig.9
57251	11	31802 – 31844	43	M	Fig.9
57251	12	36030? – 36065?	36?	Λ	Fig.10
57251	13	38027 – 38080	54	M	Fig.9
57251	14	39385 – 39430	46	Λ	Fig.10
57251	15	40571 – 40600	30	Λ	Fig.10
57251	16	44775 – 44820	46	M	Fig.9
57251	17	46880 – 46940	61	?	Fig.12
57251	18	50630? – 50675	46?	Λ	Fig.10
57251	19	52720 – 52760	41	Λ	Fig.10
57251	20	54076 – 54115	40	M	Fig.9
57251	21	54580 – 54612	33	Λ	Fig.10
57251	22	56295 – 56343	49	M	Fig.9
57251	23	56892 – 56925	34	Λ	Fig.10
57251	24	58188 – 58210	23	Λ	Fig.10
57251	25	59745 – 59772	28	Λ	Fig.10
57251	26	62310 – 62355	46	?	Fig.12
57252	1	4667 – 4726	60	M	Fig.9
57252	2	8015 – 8080	66	M	Fig.9
57252	3	10750 – 10800	51	?	Fig.12
57252	4	13605? – 13640?	36?	?	Fig.12
57252	5	16618 – 16666	49	Λ	Fig.10
57252	6	17472 – 17502	31	Λ	Fig.10
57252	7	19175? – 19210?	36?	?	Fig.12
57252	8	24220 – 24260	41	?	Fig.12
57252	9	25960 – 25990	31	?	Fig.12
57252	10	26585 – 26620	36	?	Fig.12
57252	11	28122 – 28160	39	M	Fig.9
57252	12	29195 – 29215	21	Λ	Fig.10
57252	13	31375 – 31416	42	M	Fig.9
57252	14	32296 – 32320	25	Λ	Fig.10
57252	15	33455? – 33470?	16?	Λ	Fig.10
57252	16	34198 – 34245	48	Λ	Fig.10
57253	1	3035? – 3075?	41?	?	Fig.12
57253	2	4210 – 4235	26	?	Fig.12
57253	3	7010 – 7060	51	?	Fig.12
57253	4	9950? – 9985?	36?	?	Fig.12
57253	5	21426 – 21480?	55?	?	Fig.12
57253	6	22665? – 22700?	36?	?	Fig.12

Note: "?" indicates the uncertainty in the start–end pulse numbers, duration and classification.

(MJD 57130), and long observations of PSR B0919+06 were made in 2015 July and August (MJD 57215 – 57253, see Table 1).

3 DATA ANALYSIS AND RESULTS

A few steps were needed to analyze the recorded data. First, the radio frequency interference (RFI) was cleaned. RFI appears in a few channels for a long time or in many channels for a some short time. The polluted data were identified and then replaced with randomly selected samples from the same channel or nearby channels to keep the statistical properties. The total power data from all channels were dedispersed with the known dispersion measure value of PSR B0919+06, and then summed with proper weights due to different gains of the 256 or 128 channels to get a long time series. Finally, the individual pulses were aligned with the best period which we found out around the formal period value.

Results from a test observation of PSR B0919+06 on MJD 57130 are shown in Figure 2. One abnormal emission event was identified between pulses 365 and 395, as illuminated in the right panels, in which pulses show up at earlier phases of about 5° in longitude. This event is very similar to the two abnormal emission events observed by Rankin et al. (2006, shown in their Figure 1) and the one "main flare state" observed by Perera et al. (2015, shown in their Figure 10), during which individual pulses have a gradual shifting in the pulse rotation phase for 30-40 periods.

To investigate how often such events occur, we have carried out observations in 5 days, several hours in each day. The aligned

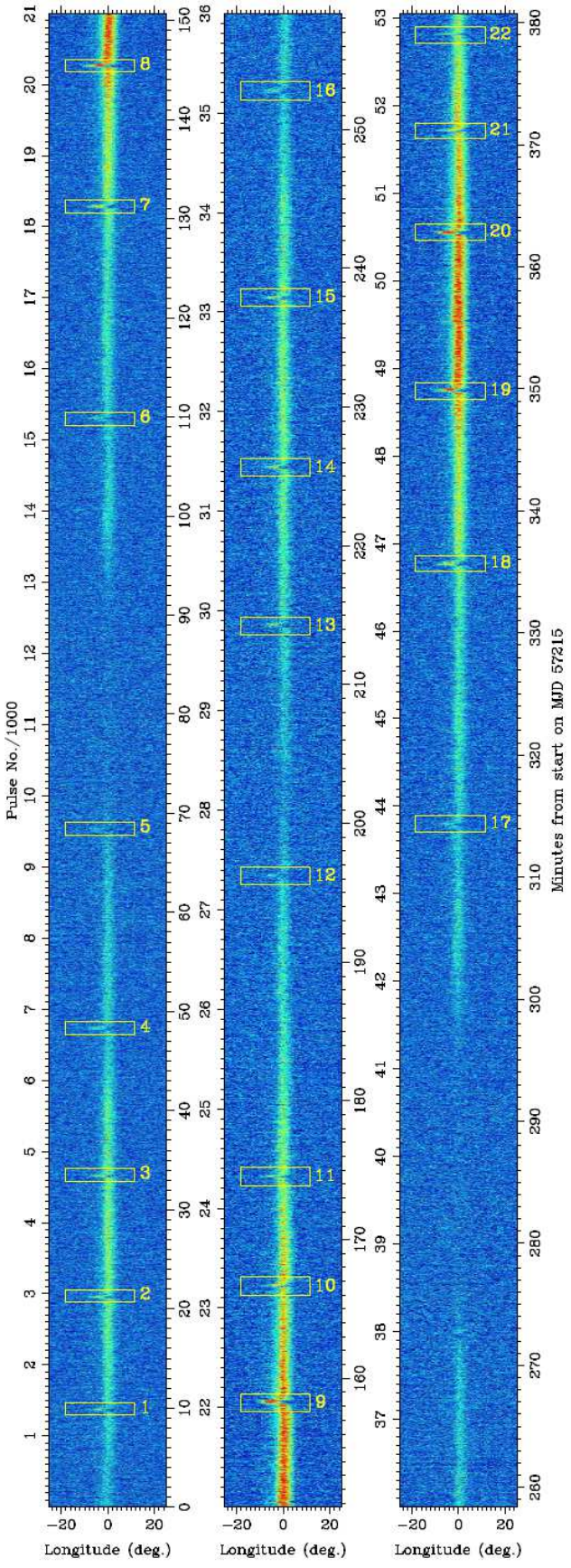

Figure 3. The 53,053 individual pulses observed on MJD 57215, in which 22 abnormal emission events are seen as indicated by the boxes.

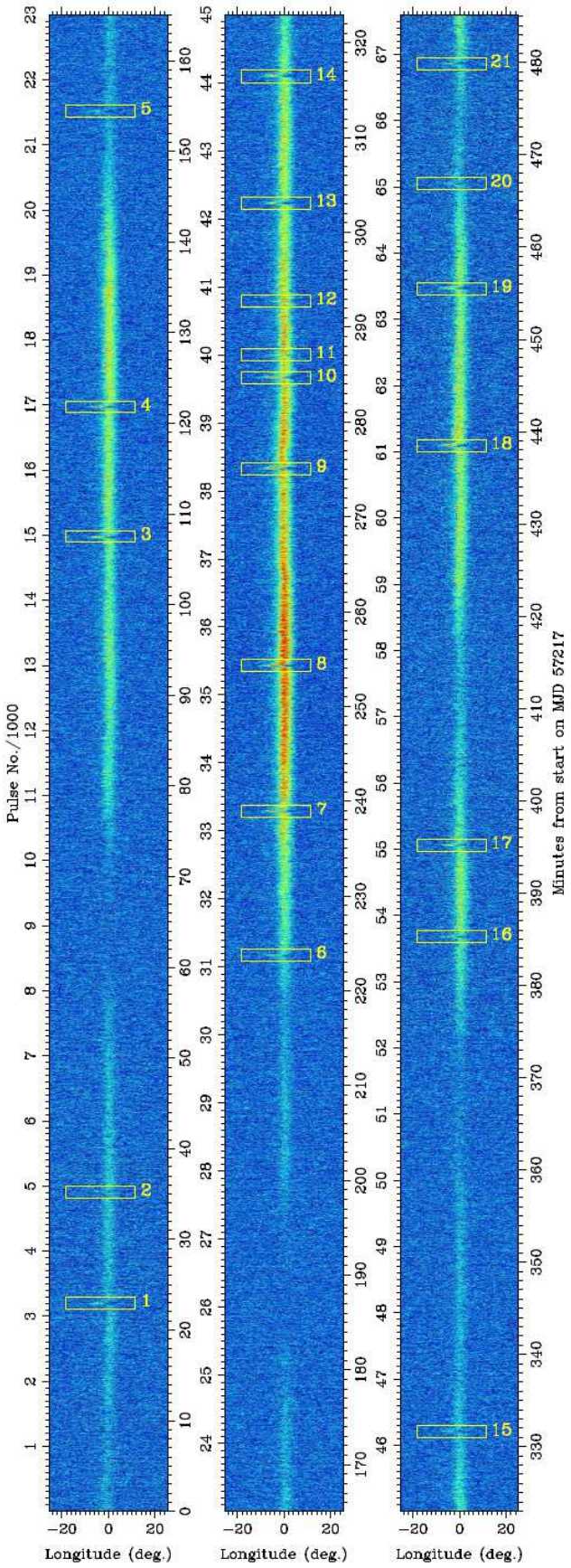

Figure 4. The same as Fig.3 but for 67,611 individual pulses observed on MJD 57217 and the 21 abnormal emission events.

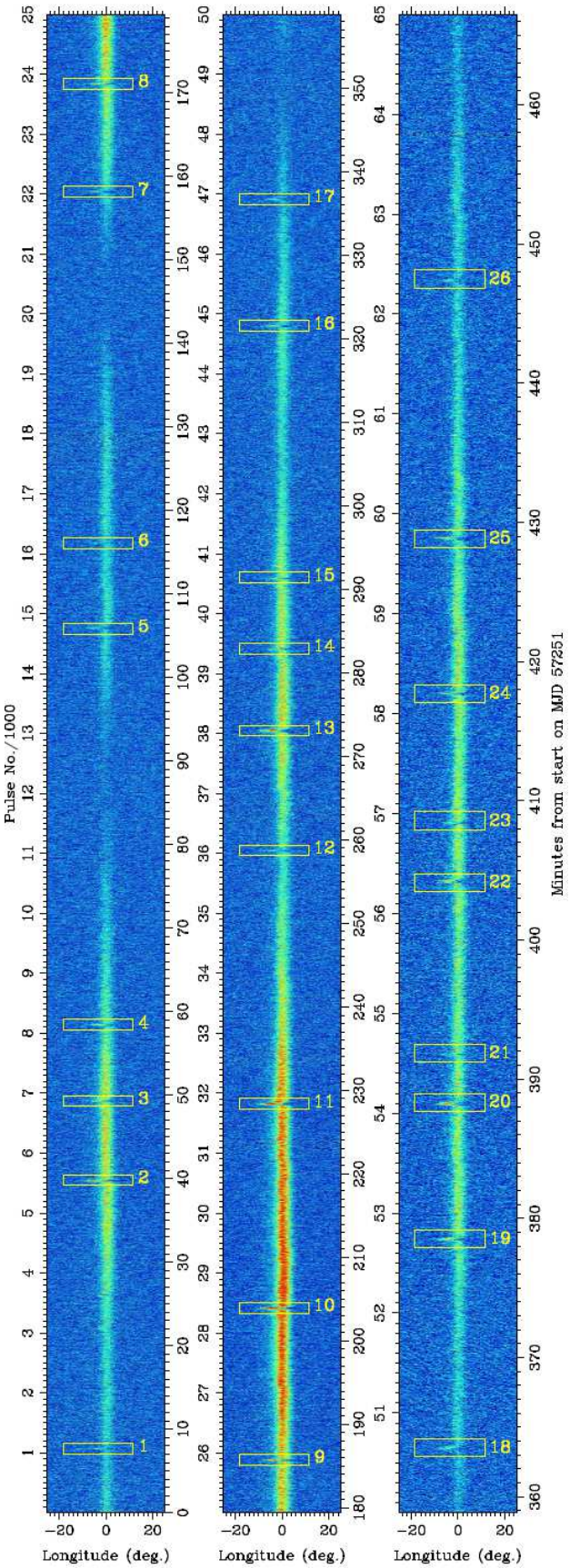

Figure 5. The same as Fig.3 but for 65,003 individual pulses observed on MJD 57251 and 26 abnormal emission events.

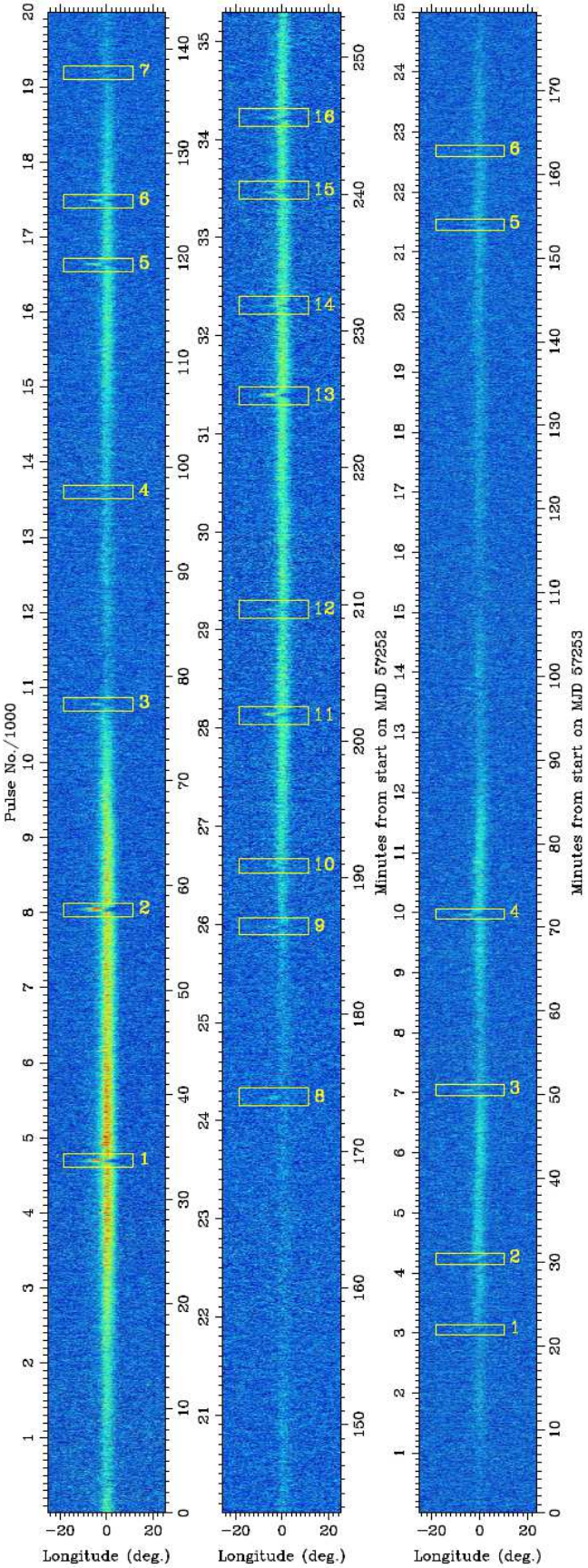

Figure 6. The same as Fig.3 but for 35,306 individual pulses observed on MJD 57252 and 25,001 pulses observed on MJD 57253, in which 16 and 6 abnormal emission events are found, respectively.

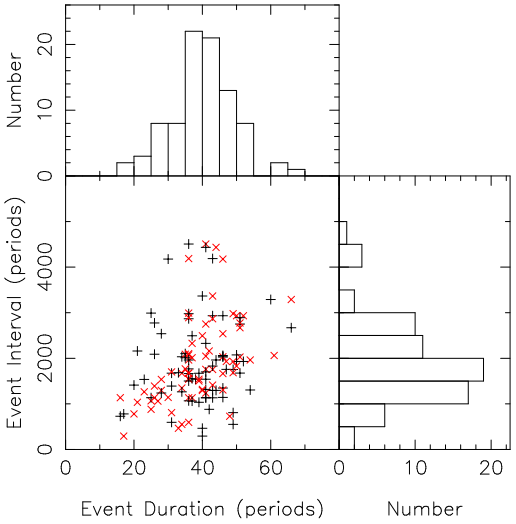

Figure 7. Duration statistics for the normal emission mode and abnormal emission events of PSR B0919+06. When the signal-to-noise ratio is good enough to count individual pulses, the period number of an abnormal emission event is taken as the horizontal value in the main panel, and the period number of the normal emission mode ahead of (or after) the event is taken as the vertical value, so that a point is plotted as "+" (or "×"). The histograms on the top panel and the right panel show pulse number distribution of abnormal emission events and the event intervals, respectively.

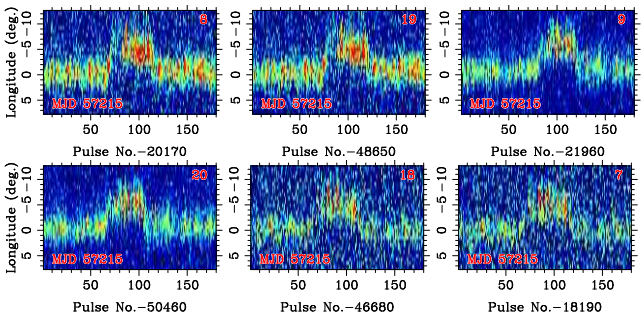

Figure 8. The detailed plots for 6 abnormal emission events of "ΠI type". The pulse number is plotted on the horizontal axis, and the longitude for the pulse phase on the vertical axis. The flux intensity of pulses is represented in colors with the dark color for zero and bright color for high intensity. MJD and the event number are indicated in each plot.

plots of individual pulses[1] are shown in Figures 3–6. Due to interstellar scintillation, the flux intensity of PSR B0919+06 clearly shows variations on a time scale of one to two hours. From these long series of individual pulses, we found 92 abnormal emission events through the visual-checking of plots. See Table 2 for their start and end pulse numbers. Based on the total number of events over the entire timespan of observations, we can estimate that one event, on average, occurs about every 20 minutes. However, there are possibilities that events were missing when pulsar signals are weaked by scintillation. The total number of events should therefore be taken as the lower limit, and hence the waiting time of events are expected to be shorter. As shown in Figure 7, we made the duration statistics for the pulsar normal mode emission and abnormal emission events. The abnormal emission events were seen to last for 15–70 periods with a peak of about 40 periods (i.e. $\leqslant$20

[1] Dedispersed data series are available at http://zmtt.bao.ac.cn/psr-jms/

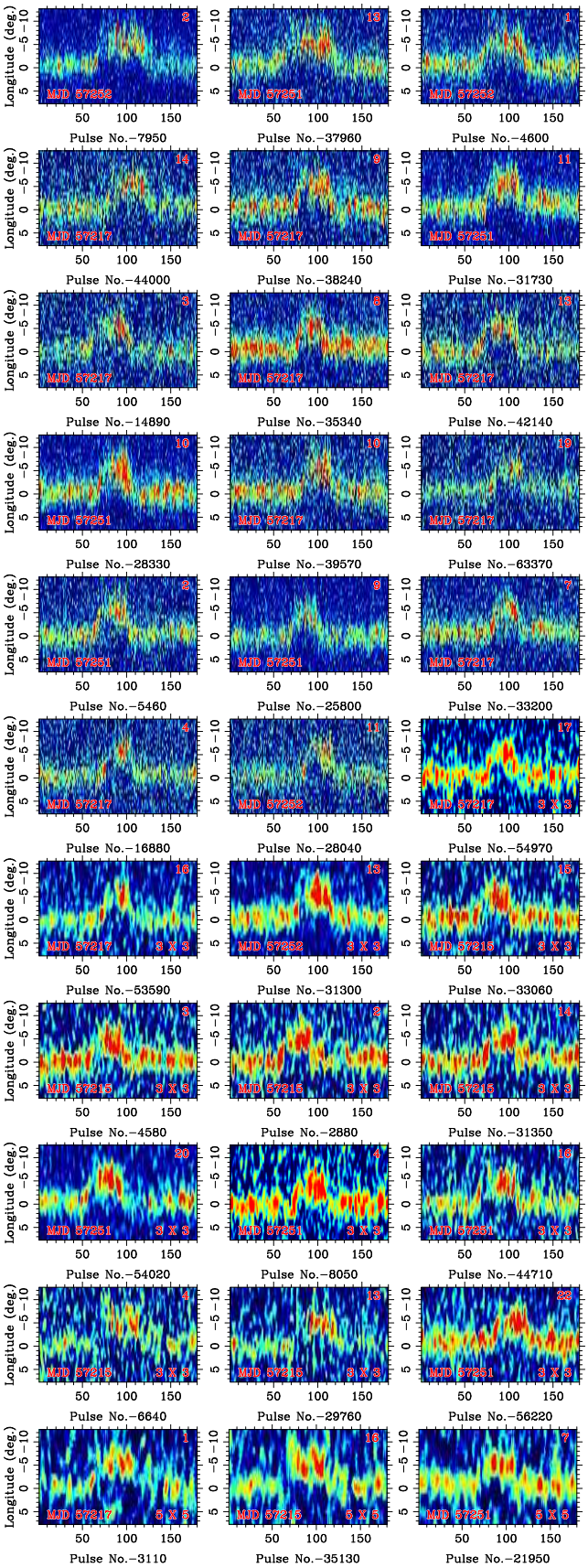

Figure 9. The detailed plots for abnormal emission events of "M type". For events with a weak signal-to-noise ratio, the "images" are enhanced by a Gaussian smooth of 3×3 pixels or 5×5 pixels.

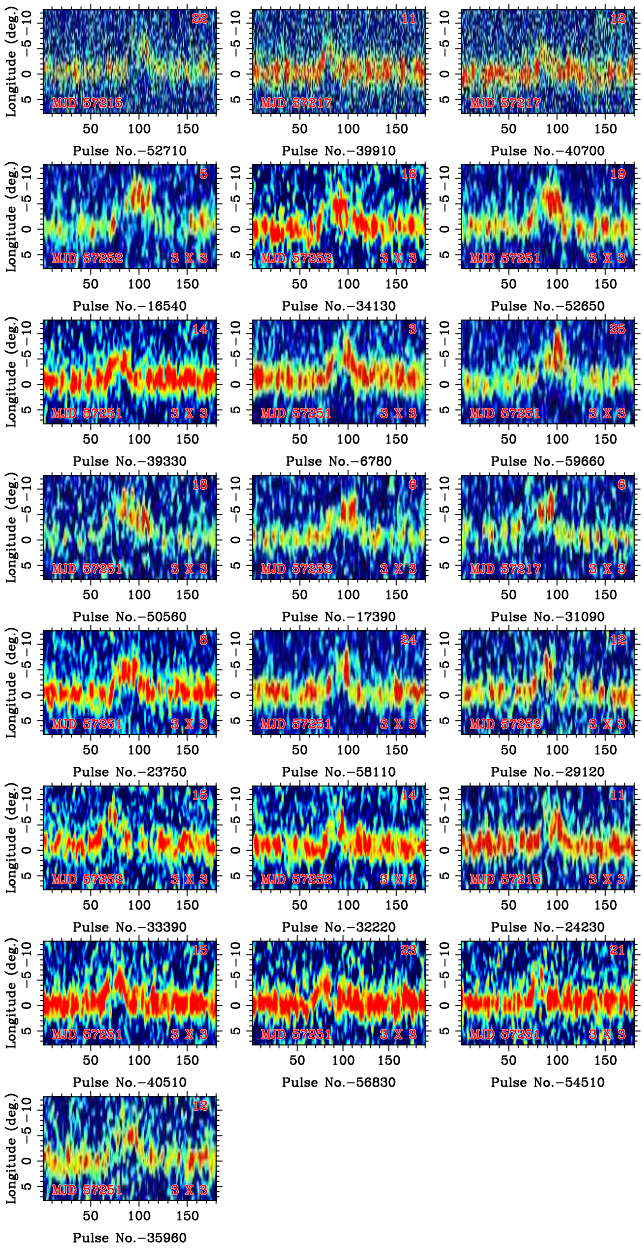

Figure 10. The detailed plots for abnormal emission events of "Λ type", including some "small flares". Most "images" have been enhanced.

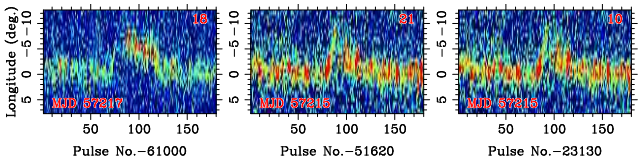

Figure 11. The detailed plots for abnormal emission events of "λ type".

seconds, remembering the pulsar period of 0.43062 s), and normal emission lasted for 1000 to 3000 periods with a peak about 1500 periods (i.e. ∼10 minutes).

The abnormal emission events of PSR B0919+06 were obviously detected by looking at plots for individual pulses if with a good signal-to-noise ratio. For events with weak signals, the data samples of neighbor phase bins and from a few periods could be

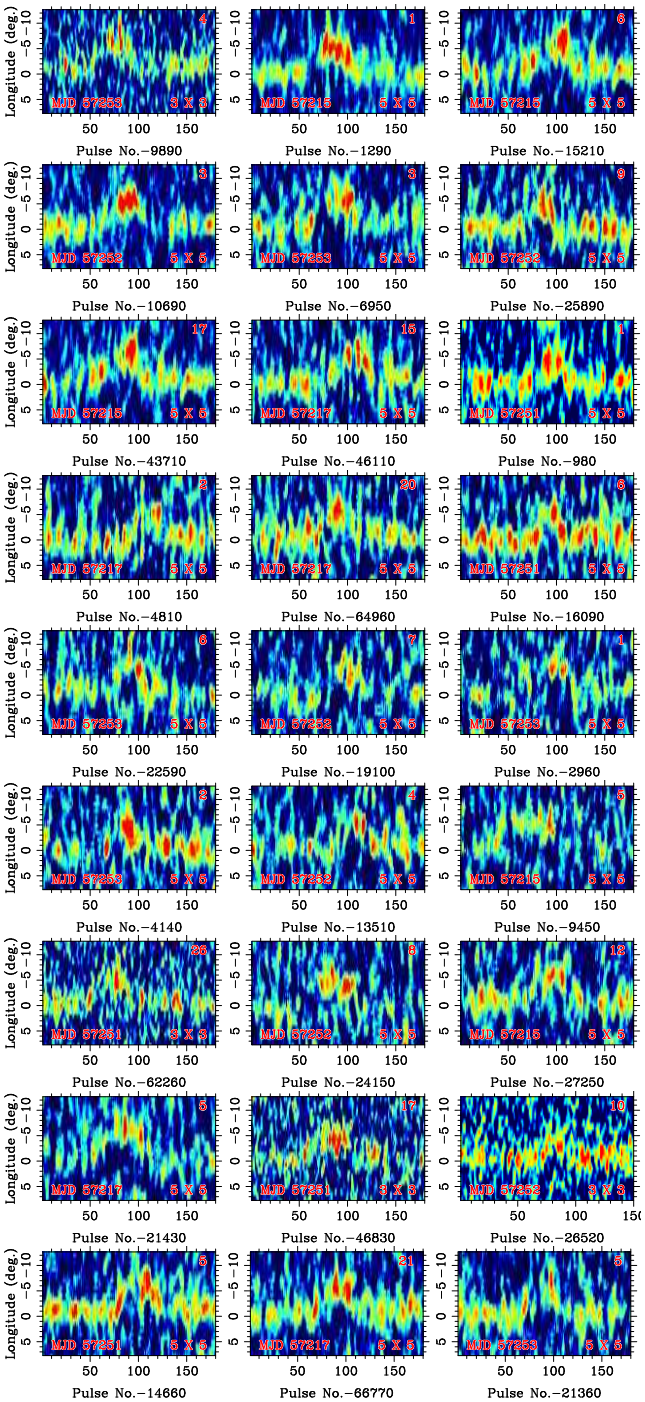

Figure 12. The detailed plots for unclassified weak abnormal emission events. All "images" have been enhanced.

averaged to enhance the signal-to-noise radio. Based on their details of phase-shifting of individual pulses, we classified abnormal emission events as following:

- Π **type:** Individual pulses of abnormal emission events abruptly come a few degrees early in longitude, and then stay in this phase range (i.e. the "high state") for a few tens of periods, eventually come back abruptly to the normal phase range. There are seven such cases detected during our observations, one shown in Figure 2 and six shown in Figure 8. Such a quick switching is almost the same as the mode-changing phenomena of other pulsars.

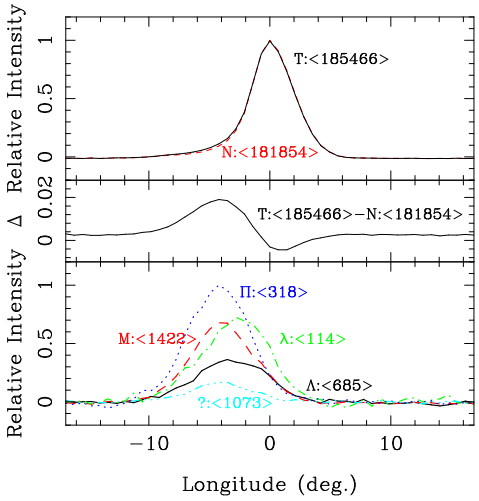

Figure 13. Comparison of profiles for the normal emission mode and abnormal emission events. On the top panel the mean profile of 181854 normal emission pulses are compared with all 185466 pulses including 3612 pulses in the abnormal emission events. The difference of their normalized profiles is shown in the middle panel. In the lower panel, the mean profiles are presented for 318 individual pulses from the Π type, 1422 pulses from the M type, 685 pulses from the Λ type, 114 pulses from the λ type of abnormal events are shown, together with the mean profile from the 1073 weak pulses from the unclassified events, which are all offset from the normal pulses.

Note also that subpulse drifting was observed before and during the abnormal emission events No. 8 and No. 19 observed on MJD 57215, which can be seen from very enlarged plots of Figure 8.

- **M type**: It is the original type of abnormal emission event that was discovered by Rankin et al. (2006). Individual pulses gradually "go up" on the longitude over a few periods, stay on the "high state" for more than 20 periods perhaps with some fluctuations in phases, and finally gradually come back to the normal phase over a few periods. We identified 33 events of this type (see Figure 9).
- Λ **type**: Individual pulses of this type of events rise and fall gradually without staying in the "high state". We identified 22 events of this type (shown in Figure 10). Some of the events were the "small flares" as these seen by Perera et al. (2015).
- λ **type**: A few abnormal emission events show a rapid "rise" but a slow "decay", which appears as a longer tail in Figure 11.

In addition to these classified events, 26 events (see Figure 12) have a very weak signal-to-noise ratio, which can not be certainly classified even after their "images" are enhanced by a "Gaussian smoothing". These events are marked with a "?" for the type in Table 2.

The short duration and the small total number of individual pulses of abnormal emission events indicates that they contribute very little ($\sim 2\%$) to the mean intensity. In Figure 13, we compare the mean pulsar profile from all 185466 bright pulses including abnormal emission events with that from 181854 bright pulses excluding the abnormal emission events in between. The difference between the above two profiles are shown in the middle panel. In the bottom panel the mean profiles of all types of abnormal emission events are shown, and clearly they are different. The abnormal emission events mostly affect the mean profile in the phase window of -2° to -8°.

4 DISCUSSIONS AND CONCLUSIONS

We observed PSR B0919+06 for about 30 hours and detected 92 abnormal emission events during which individual pulses are shifted to early pulse phases by a few degrees in longitude. Such events last for a few tens of periods, and are seen to happen randomly every 1000 to 3000 periods. We have classified the abnormal emission events into four types based on the phase-shift features of individual pulses.

Although the pulse number during the abnormal emission events are small (3612 vs. 185466 normal pulses, i.e. about 2%), it is clear that the abnormal emission events should lead to changes of mean pulse profiles of PSR B0919+06 up to 2%. This amplitude is roughly equal to the difference of the two profile modes shown by Perera et al. (2015). Timing observations for 20 minutes or less may or may not include one abnormal emission event, since the events occur randomly with an interval of 500 to 3500 periods (i.e. 200 to 1400 seconds). Therefore it is not clear if the long-term variations of profiles are related to such abnormal emission events. In addition, during timing, it seems to be important to get the time of arrival of pulses by fitting the standard profile to the profiles only in the later phase range of $> -1^\circ$, rather than the all phase ranges of pulsed emission.

Can the precession be the causal reason for the abnormal emission events? Free precession has been suggested to cause long-term variations of pulsar profiles and $\dot{\nu}$ (Stairs et al. 2000; Kerr et al. 2015), especially their correlation (Akgün et al. 2006; Jones 2012). However, a small wobbling of the rotation axis should lead a gradual variation of profiles quasi-periodically, not just in short duration of 20 seconds of every 10 to 15 minutes. Therefore, it is very unlikely that the precession is the intrinsic cause for such abnormal emission events lasting only for a few tens of periods.

We emphasize that PSR B0919+06 is not the only pulsar with such a phase shift. PSR B1859+07 was also found (Rankin et al. 2006; Perera et al. 2016) to exhibit similar events, though the events were seen to be much more frequent. Other pulsars might have similar emission features uncovered, simply due to lack of long observations.

Based on the features of abnormal emission events of PSR B0919+06 we observed, together with the same mean "S"-shaped curve of polarization angles of the abnormal emission events as the normal trailing conal component observed by Rankin et al. (2006, as described in Section 1), we believe that the abnormal emission events of PSR B0919+06, as the phenomena of mode-changing and subpulse drifting observed in other pulsars, probably originate from emission processes in the pulsar magnetosphere.

ACKNOWLEDGMENTS

We thank Prof. JinXin Hao of NAOC for his support of this work, Prof. Biping Gong from Huazhong University of Science and Technology for stimulative discussions, and Ms. SuSu Shan, Mr. Fan Yang and the operation team of Jiamusi 66 m Deep Space Station of the China Xi'an Satellite Control Center for the assistance of observations. We also thank the referee for helpful comments. The authors are partially supported by the National Natural Science Foundation of China through grants No. 11473034 and 11273029, the Strategic Priority Research Program "The Emergence of Cosmological Structures" of the Chinese Academy of Sciences, Grant No. XDB09010200, and the Open Fund of the State Key Laboratory of Astronautic Dynamics of China.

REFERENCES

Akgün T., Link B., Wasserman I., 2006, MNRAS, 365, 653
Gangadhara R. T., Gupta Y., 2001, ApJ, 555, 31
Gil J. A., Jessner A., Kijak J., Kramer M., Malofeev V., Malov I., Seiradakis J. H., Sieber W., Wielebinski R., 1994, A&A, 282, 45
Hankins T. H., Rankin J. M., 2010, AJ, 139, 168
Hobbs G., Hollow R., Champion D., et al. 2009, PASA, 26, 468
Johnston S., Karastergiou A., Mitra D., Gupta Y., 2008, MNRAS, 388, 261
Jones D. I., 2012, MNRAS, 420, 2325
Kerr M., Hobbs G., Johnston S., Shannon R., 2015, MNRAS, in press. ArXiv e-prints 1510.06078
Latham C., Mitra D., Rankin J., 2012, MNRAS, 427, 180
Lyne A., Hobbs G., Kramer M., Stairs I., Stappers B., 2010, Science, 329, 408
Lyne A. G., Manchester R. N., 1988, MNRAS, 234, 477
Manchester R. N., 1995, Journal of Astrophysics and Astronomy, 16, 107
Perera B. B. P., Stappers B. W., Weltevrede P., Lyne A. G., Bassa C. G., 2015, MNRAS, 446, 1380
Perera B. B. P., Stappers B. W., Weltevrede P., Lyne A. G., Rankin J. M., 2016, MNRAS, 455, 1071
Phillips J. A., Wolszczan A., 1992, ApJ, 385, 273
Rankin J. M., 1986, ApJ, 301, 901
Rankin J. M., Rodriguez C., Wright G. A. E., 2006, MNRAS, 370, 673
Rankin J. M., Wright G. A. E., Brown A. M., 2013, MNRAS, 433, 445
Smits J. M., Stappers B. W., Edwards R. T., Kuijpers J., Ramachandran R., 2006, A&A, 448, 1139
Sobey C., Young N. J., Hessels J. W. T., et. al. 2015, MNRAS, 451, 2493
Stairs I. H., Lyne A. G., Shemar S. L., 2000, Nat, 406, 484
Stinebring D. R., Cordes J. M., Rankin J. M., Weisberg J. M., Boriakoff V., 1984, ApJS, 55, 247
Wang N., Manchester R. N., Johnston S., 2007, MNRAS, 377, 1383
Wang P. F., Han J. L., Wang C., 2013, ApJ, 768, 114
Yang A., Han J. L., Wang N., 2014, Science China Physics, Mechanics, and Astronomy, 57, 1600